CORRELATION BETWEEN DROP VAPORIZATION AND AUTOIGNITION PHENOMENA

S.M. Frolov[1], V.Ya. Basevich[1], F.S. Frolov[1], A.A. Borisov[1], V.A. Smetanyuk[1], B. Basara[2], P. Priesching[2], and R. Tatschl[2]

[1]*SEMENOV INSTITUTE OF CHEMICAL PHYSICS, MOSCOW, RUSSIA*

[2]*AVL LIST GMBH, GRAZ, AUSTRIA*

Abstract: Based on the detailed parametric study of drop vaporization and autoignition in suspensions, a local autoignition criterion based on the approximate heuristic invariance of the normalized ignition distance have been suggested.

Introduction

The classical theory of liquid drop vaporization, ignition, and combustion considers an isolated drop in unconfined ambience [1–4]. Within this presumption, notable progress in understanding relevant physical and chemical processes has been achieved recently [5–8]. However, in practice, these processes occur in presence of neighboring drops. The corresponding effects are usually referred to as 'spray' effects. Spray effects manifest themselves in two-phase reactive flows [9–15]. In existing computational approaches, chemical reaction rates are determined based on considering homogeneous gas-phase autoignition and combustion with fuel drops treated only as source terms for fuel vapor. As a matter of fact, spray autoignition and combustion are complex combinations of localized ignition events in the inhomogeneous mixture and diffusion-controlled flames around individual drops, groups of drops, and gas-phase partially premixed flames.

The objective of this study was to elaborate the drop autoignition criterion based on detailed modeling of drop vaporization and ignition with spray effects taken into account.

Formulation

For a spatially uniform and monodisperse drop suspension in air, an elementary cell in the form of hexahedron (in a plane, see Figs. 1*a* and 1*b*) or polyhedron with faces in the form of equilateral triangles (in space, see Fig. 1*c*) can be constructed around each drop [16].

The length of a polyhedron edge is equal to a half-distance between drops in suspension, R_c. Due to symmetry considerations, mass, momentum, and energy fluxes through the faces will be zero. Polyhedron volume, V_s, and surface area, S_c, are:

$$V_c = \frac{5\sqrt{2}}{3} R_c^3, \qquad S_c = 5\sqrt{3} R_c^2$$

Thus, drop behavior in the suspension can be modeled by solving the governing conservation equations for a single drop with symmetry boundary conditions at the polyhedron faces. As shown in [16, 17] based on three-dimensional (3D) simulation of laminar flow pattern around an evaporating drop, the polyhedron cell can be approximated with an elementary sphere. In this case, the 3D problem is reduced to one-dimensional formulation with zero-flux boundary conditions at the surface of the elementary sphere of radius, R, equal to

$$R = \left(\frac{5\sqrt{2}}{4\pi} \right)^{1/3} \cdot R_c \approx 0.826 R_c$$

The volume of the elementary sphere is $V = V_c$ and the surface area is $S / S_c \approx 0.99$. The error of such an approximation depends on the suspension density (loading ratio η — mass of dispersed liquid in the unit volume). At a given loading ratio, the radius of the elementary sphere is equal to

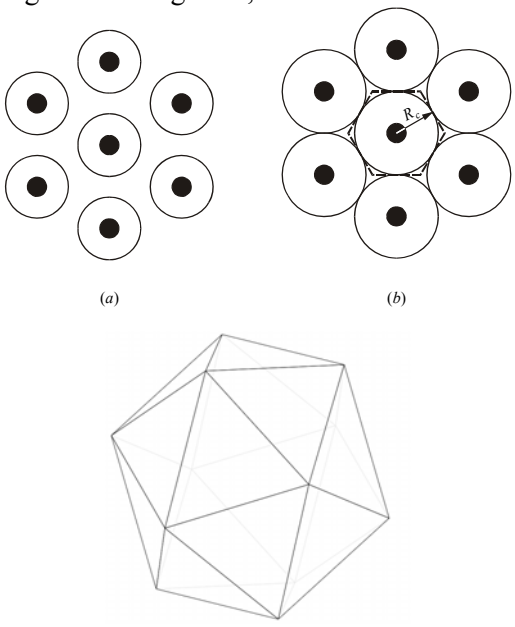

Fig. 1: Elementary cell for the uniform monodisperse drop suspension [16]. Black circles denote drops. Circumferences around drops characterize the spread of diffusion fluxes from individual drops. (*a*) Spray effects are absent; (*b*) spray effects manifest themselves. Dashed line in (*b*) bounds the elementary cell with zero mass and energy fluxes through its surface; R_c is the characteristic cell size (half-distance between drops; (*c*) three-dimensional elementary cell in the form of regular polyhedron with 20 faces.

$$R \approx r_0 \left(\frac{\rho_l}{\eta} \right)^{1/3}$$

where r_0 is the initial drop radius and ρ_l is the liquid density. In terms of the equivalence ratio, $\Phi = \eta / (\phi_{st} \rho_g)$, the radius of the elementary sphere is equal to

$$R \approx r_0 \left(\frac{\rho_l}{\rho_g \Phi \phi_{st}} \right)^{1/3}$$

where ρ_g is the initial gas density and ϕ_{st} is the stoichiometric fuel–air ratio. At normal atmospheric conditions, for stoichiometric mixtures of liquid hydrocarbon fuels $\rho_g = 1.19$ kg/m^3, $\rho_l = 700 - 800$ kg/m^3, $\phi_{st} \approx 0.06$, and $\Phi = 1$, therefore $\eta = \eta_{st} \approx 0.07$–$0.08$ kg/m^3, $R_c / r_0 \approx 25 - 27$ and $R / r_0 \approx 21 - 22$. At elevated pressure, for example at the end of compression stroke in a Diesel engine, ($\rho_g \approx 30$ kg/m^3) $R_c / r_0 \approx 9$ and $R / r_0 \approx 8$.

The mathematical statement of the problem is based on the following simplifying assumptions: (1) the drop is immovable and has a spherical shape, (2) no internal diffusion of species and

convection exists inside the drop, (3) buoyancy effects in the gas phase are not considered, (4) pressure is constant, and (5) concentration of fuel vapor at the drop surface is governed by the equilibrium relationship. The governing equations of the model include the partial differential equations of energy conservation in the drop; gas-phase continuity and energy conservation equations; multicomponent diffusion equations for gas-phase species, and the real-gas equation of state for the gas phase. All relevant physical processes are considered as functions of pressure and temperature.

Boundary conditions comprise the symmetry condition in the drop center; temperature, heat and mass flux continuity conditions at the drop surface; and the zero gradient conditions at the spherical elementary cell surface. As the model implies constant pressure, the radius of the elementary sphere is dependent of time, i.e., $R = R(t)$. The expansion/shrinking of the sphere is found from the solution by allowing the external boundary of the sphere to move with the gas at a radial distance of $r = R$. Initial conditions encounter homogeneous conditions inside and outside the drop.

Gas-phase oxidation of hydrocarbon fuel is modeled by means of the overall reaction mechanism preliminarily validated for propagating premixed flames, nonpremixed counterflow flames, single drop autoignition and diffusion flames [18–22].

Results and Discussion

Numerical solution of mass, momentum, and energy conservation equations for a hydrocarbon drop within the elementary sphere resulted in several important findings. Below these findings are discussed on examples of drop vaporization and autoignition.

Drop Vaporization in Suspension

Analysis of drop vaporization in dense drop suspensions indicates that drop lifetime increases considerably as compared to the isolated drop in an unconfined atmosphere. Figure 2 shows the calculated time histories of the normalized squared drop diameter ($d_0 = 2r_0$ is the initial drop diameter) depending on Φ. Three important findings are worth mentioning: (1) at larger Φ drops evaporate slower, (2) the deviations from the classical d^2-law increase as Φ increases,

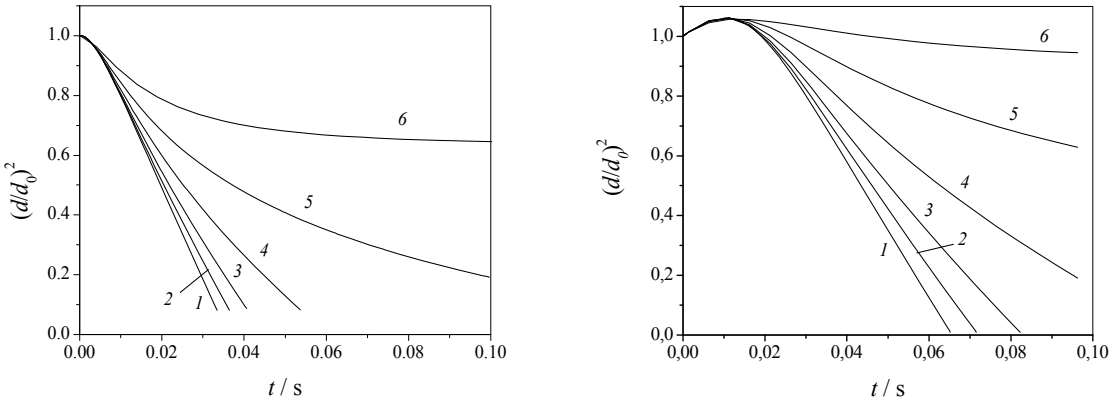

Fig. 2: Predicted time histories of normalized surface of an *n*-heptane (*a*) and *n*-tetradecane (*b*) drop evaporating in air as a function of Φ [16]. Initial parameters: drop diameter $d_0 = 70$ μm, drop temperature $T_{l0} = 293.15$ K, gas temperature $T_{g0} = 573.15$ K, and pressure $p = 0.1$ MPa. (*a*): *1* — $\Phi = 0$ (isolated drop), *2* — 1.06, *3* — 2.12, *4* — 4.25, *5* — 8.5, and *6* — 17.0; (*b*): *1* — $\Phi = 0$ (isolated drop), *2* — 0.6, *3* — 1.2, *4* — 2.4, *5* — 4.75, and *6* — 9.5

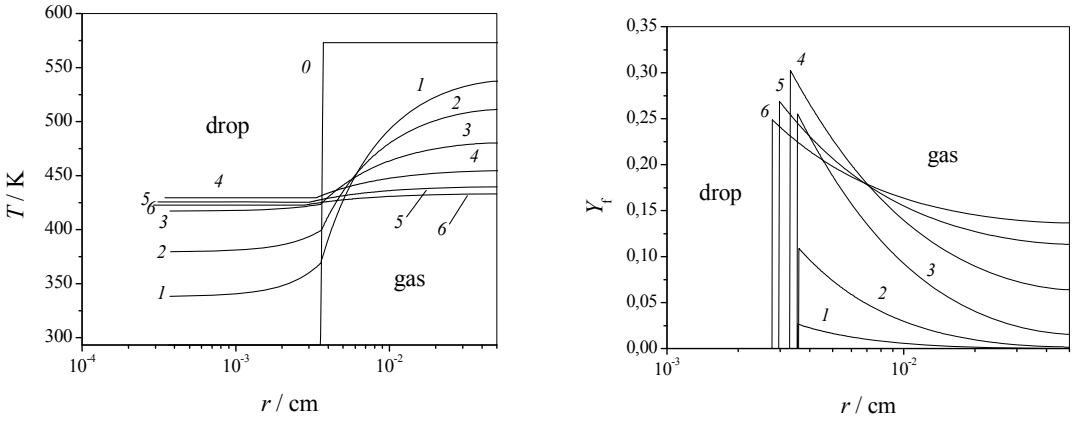

(*a*) (*b*)

Fig. 3: Predicted evolution of temperature (*a*) and fuel mass fraction (*b*) profiles at evaporation of *n*-tetradecane drop in air. Initial parameters: $d_0 = 70$ μm, $T_{l0} = 293.15$ K, $T_{g0} = 573.15$ K, $p = 0.1$ MPa, and $\Phi =$ 4.75; *0* – $t =$ 0; *1* — 5 ms, *2* — 10 ms, *3* — 20 ms, *4* — 40 ms, *5* — 70 ms, and *6* — 95 ms.

and (3) drops evaporate only partly starting from a certain Φ. The latter finding is due to considerable screening effect of neighboring drops in the cloud resulting in fast temperature decrease in the elementary sphere (Fig. 3*a*) and a vapor saturation conditions (Fig. 3*b*) in the interdrop space. Slower vaporization of individual drops has been observed in experiments with linear drop arrays [23].

Drop Autoignition in Suspension

When fuel drops are injected in high-temperature oxidizing atmosphere they can autoignite after a certain time period referred to as the ignition delay t_i. The localized autoignition of fuel vapor occurs at a certain distance from the drop surface (Fig. 4). The ignition delay t_i is usually defined as the time taken for the maximum rate of temperature rise to attain a certain preset value, e.g., $T'_{\max} = 10^6$ K/s or 10^7 K/s. All rational definitions usually lead to very close values of t_i

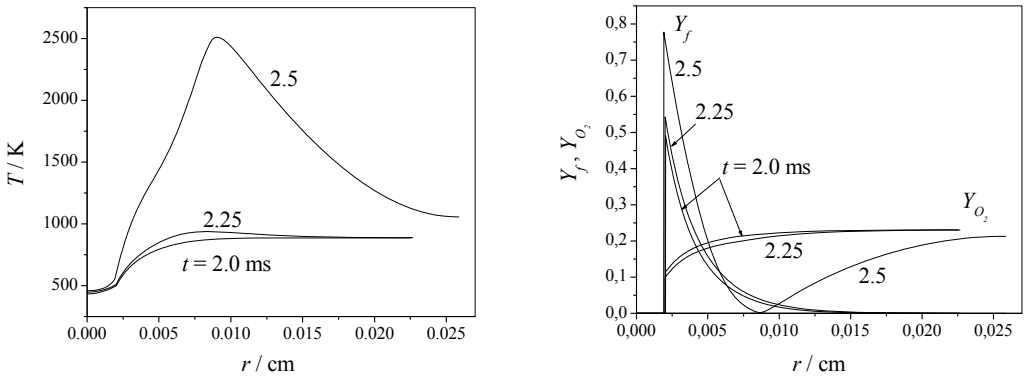

(*a*) (*b*)

Fig. 4: Predicted evolution of temperature (*a*) and fuel and oxygen mass fractions (*b*) profiles at autoignition of *n*-decane drops in air. Initial parameters: $d_0 = 40$ μm, $T_{l0} = 300.15$ K, $T_{g0} = 900.15$ K, $p = 2.0$ MPa, and $\Phi = 1.0$

Table 1: Comparison of predicted and measured ignition delays for isolated *n*-heptane drops at pressure 0.1 MPa and initial drop temperature 293 K in microgravity conditions.

Initial drop diameter, μm	Air temperature, K	t_i, s	
		Meas.	Calc.
700	1000	0.30 [26]	0.19
1000	960	0.58 [27]	0.48

Table 2: Reaction mechanism.

Reaction number	Reaction
1	$C_nH_m+(0.5n+0.25m)O_2 \rightarrow nCO+0.5mH_2O$
2	$H_2+H_2+O_2 \rightarrow 2H_2O$
3	$CO+CO+O_2 \rightarrow CO_2+CO_2$
4,-4	$CO+H_2O \leftrightarrow CO_2+H_2$

Detailed calculations of *n*-heptane drop autoignition were reported in [22, 24, 25]. For isolated drops in the microgravity conditions a good agreement of predicted and measured ignition delays was obtained (Table 1). The radius of the elementary sphere R was taken sufficiently large as compared to the initial drop radius r_0, so that the parameters at the edge of the elementary sphere remained constant in the course of calculations.

The overall oxidation mechanism for hydrocarbons studied herein is presented in Table 2.

The mechanism of chemical transformations determining the energy release rate at fuel oxidation was represented by the (well validated) overall reaction mechanism containing 6 species and 5 reactions. The rate of reactions was determined as

$$w_{ij}=A_{ij}\,P^{mij}\exp(-E_{ij}/RT)\Pi\, n_j,$$

where A_{ij} is the preexponential factor, E_{ij} is the activation energy, and R is the gas constant. Note that reaction #1 was treated as the bimolecular reaction between fuel and oxygen. Table 3 shows the values of kinetic parameters of reactions 1, 2, 3, 4, and -4 (reverse reaction) listed in Table 2 for *n*-decane and *n*-teradecane.

Table 3: Kinetic parameters of the reaction mechanism of *n*-alkane autoignition.

Reaction number	A_{ij}, liter, mole, s	m_{ij}	E_{ij} kcal/mol	Remark
1	3.5+13	0	36.7	n-decane
1	1.75+14	0	36.7	n-tetradecane
2	7.0+13	-0.5	21.0	
3	8.5+12	-1.5	21.0	
4	1.0+12	-1.0	41.5	
-4	3.1+13	-1.0	49.1	

Application of the methodology described above for calculating the ignition delay in Diesel engine conditions also provides satisfactory results. Figure 5 compares the predicted overall ignition delays for n-tetradecane drops of initial diameter $d_0 = 20$ μm (dashed curve) with measured ignition delays [28] for the drops of fuels with different Cetane numbers (CN).

Figure 6 compares predicted ignition delays for n-decane and n-tetradecane drops of different diameters with the values measured in Diesel engine [29]. The calculations were made for typical Diesel conditions (temperature $T_0 = 800$ K, pressure $p = 40$ bar, equivalence ratio in drop suspension $\Phi = 1.0$). The predicted ignition delays are seen to be close to those measured in the Diesel engine conditions. For more accurate comparison it is necessary to better represent the composition of Diesel oil and the drop size distribution. Moreover, it is necessary to make a calculation at variable (rather than constant) temperature and pressure.

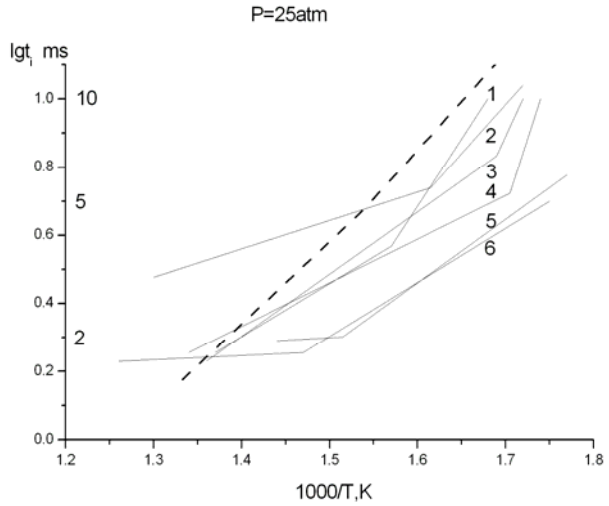

Fig. 5: Comparison of predicted (dashed curve) and measured (solid curves) ignition delays for different fuels at pressure 25 bar. Dashed curve – n-tetradecane drops with d_0 =20 μm ; Solid curves – fuels with different CN and two different spray atomizers (1 and 2): CN/Atomizer: 1 – 49/1; 2 – 50/1; 3 – 49/2; 4 – 50/2; 5 – 70/2, 6 – 62/2.

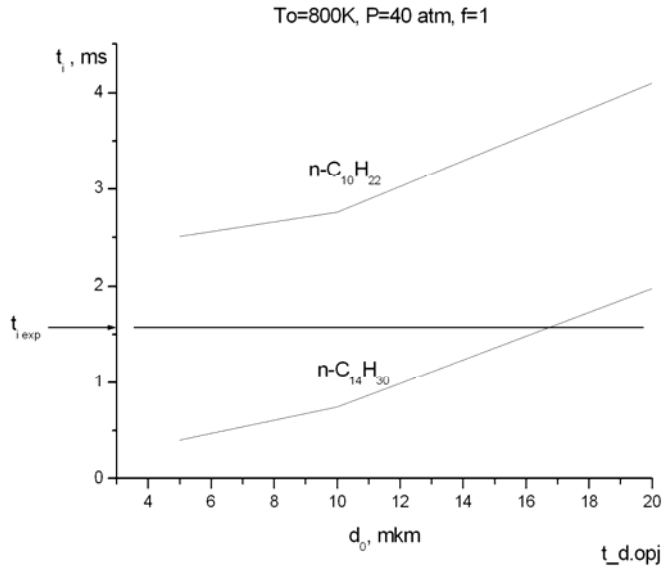

Fig. 6: Comparison of predicted and measured ignition delays at Diesel engine conditions. Calculations are made for n-decane (upper curve) and n-tetradecane (lower curve) drops of different initial diameter at 800 K, 40 bar and spray fuel – air ratio of 1.0. Horizontal line t_{iexp} = const corresponds to the measured value of ignition delay of Diesel oil at similar conditions [29].

Calculations of Ignition Delay

The computational methodology described above was used for making two sorts of comparative calculations, namely, (1) calculations of drop autoignition and combustion and (2) calculations of drop vaporization without chemical transformations. The calculations of both sorts were performed in the wide range of drop diameters (d_0=20–150 μm), suspension equivalence ratios ($\Phi = 0.1$–2.0), pressures (p = 20–80 bar), and temperatures (T_0 = 800–900 K). The fuels used were n-decane and n-tetradecane.

When making drop autoignition calculations, we purposefully monitored temperature profiles in the drop vicinity (1) before the autoignition, (2) at the instant of autoignition, and (3) at completion of localized autoignition, as shown in Fig. 4a. In the example of Fig. 4a, the instant (1) corresponds to t = 2.0 ms, instant (2) – to 2.25 ms, and instant (3) – to 2.5 ms.

Using such an approach we determined the ignition delay time t_i (approximately 2.25 ms in Fig. 4a) and the location of the autoignition site in terms of the distance from the drop center r_i (approximately 0.0085 cm in Fig. 4a). For further generalization of these data, we used the normalized distance $r_* = 2r_i / d_0$ instead of r_i. From now on, the normalized distance r_* will be referred to as the normalized autoignition radius (approximately 4.25 in Fig. 4a). One of the main findings of such calculations was the fact that the normalized autoignition radius appeared to be nearly insensitive to the governing parameters, namely, air temperature, pressure, suspension fuel – air ratio, drop size, and fuel type within the ranges investigated. In general, we have found that $r_* \approx 4-5$.

Thus, the drop ignition calculations made it possible to collect a database on ignition delay times t_i and normalized autoignition radii depending on various governing parameters of the problem.

Calculations of Drop Vaporization

After drop-ignition calculations we made a series of drop vaporization calculations with the same values of governing parameters, i.e., we have repeated all previous calculations with deactivated chemical reactions in the gas phase. The main objective of these calculations was the monitoring of the local equivalence ratio φ (differes from the suspension equivalence ratio Φ!) and normalized temperature $\theta_* = (T/T_0)_*$ at the normalized autoignition radius r_* obtained from the drop-ignition calculations. More specifically, we were interested in the values of $\varphi_* = \varphi(r_*)$ and $\theta_* = (T/T_0)_*$ at $t = t_i$.

Such an analysis was performed for numerous computational cases. It has been found that the normalized autoignition temperature varied within the range from 0.83 to 1.0 with the most probable value on the level of $\theta_* = 0.9$. The normalized autoignition equivalence ratio φ_* varied within the range from 0.25 to 2.0 with the most probable value in fuel-lean local mixture composition with $\varphi_* \approx$ 0.6.

Correlation between Drop Vaporization and Ignition

Statistical analysis of the computational data revealed some important correlations between drop-ignition and drop-vaporization calculations. Figure 7 shows the correlation between the computed values of t_i and the predicted values of t_T and t_C, where t_T is the ignition delay obtained using the $\theta_* = 0.9$ criterion in drop-vaporization calculations, and t_C is the ignition delay obtained using the $\varphi_* \approx$ 0.6 criterion in drop-vaporization calculations. It is seen from Fig. 7 that there definitely exists the approximate correlation between the values of t_i, t_T, and t_C. It is worth noting that this correlation looks universal as it is independent of fuel type (n-decane or n-tetradecane), initial drop diameter (from 5 to 150 μm), suspension equivalence ratio (from 0.1 to 2.0), initial temperature (from 800 to 900 K) and pressure (from 20 to 80 bar).

Based on this finding, the following criterion of drop autoignition in suspension can be suggested:

$$r_* \approx 4;\ \theta_* = 0.9;\ \varphi_* \approx 0.6 \qquad (2)$$

The maximum errors of Eqs. (2) are 70% and 100% in terms of temperature and local equivalence ratio, respectively, which can be treated as satisfactory for such a complex chemical kinetic phenomenon as autoignition. The error of 100% for kinetic calculations is well within the uncertainty of all available experimental data for ignition delays.

When implementing the ignition criterion of Eq. (2) in computational codes, one has to take into account some important implications discussed below. Figure 8 shows the dependencies of the ignition

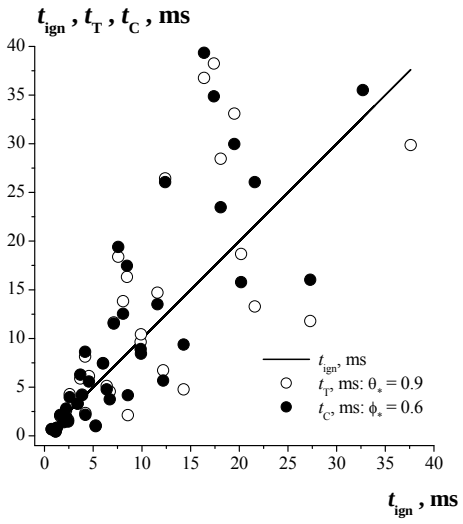

Fig. 7: Correlation between the ignition delay predicted by the drop-ignition calculations (X-axis) and the ignition delay predicted by the criteria $\theta_* = 0.9$ and $\varphi_* \approx 0.6$ based on drop-vaporization calculations.

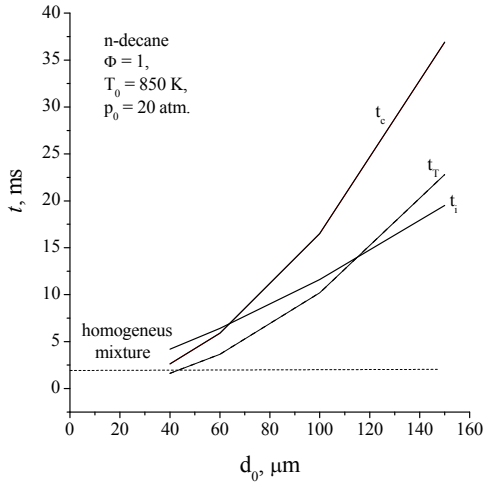

Fig. 8: Dependence of the ignition delays t_i , t_T , and t_C on the initial n-decane drop diameter at T = 850 K and p = 20 bar.

delays t_i , t_T , and t_C on the initial drop diameter. The ignition delay t_i is seen to decrease with decreasing the initial drop diameter towards the ignition delay in the homogeneous mixture (shown by the dashed horizontal line in Fig. 8) rather than to zero. Contrary to drop ignition, the homogeneous mixture is known to exhibit no diffusion-controlled slow-down of the overall reaction rate. As for the ignition delays t_T and t_C, they tend to zero because the drop vaporization time tends to zero with decreasing the initial drop size. This deficiency of the ignition criterion of Eq. (2) should be kept in mind and special measures shoud be undertaken to overcome it.

Conclusion

The detailed parametric study of drop vaporization and autoignition in suspensions made it possible to derive the local autoignition criterion based on the approximate heuristic invariance of the normalized ignition distance. The ignition criterion can be readily implemented into the multidimensional CFD codes for simulating drop cloud ignition.

Acnowledgements

This work was partly supported by ISTC (project #2740), AVL LIST GmbH (Austria), and Russian Foundation for Basic Research (grant 08-08-00068).

REFERENCES

1. Warshavskii, G. A. 1945. In: *Trans. of NII-1* 6.
2. Godsave, G. A. E. 1953. In: *4th Symposium (International) on Combustion Proceedings*, Baltimore, MD: Williams and Wilkins Co. 818–30.
3. Spalding, D. B. 1953. In: *4th Symposium (International) on Combustion Proceedings*, Baltimore, MD: Williams and Wilkins Co. 847–64.

4. Goldsmith, M., and S. S. Penner. 1954. On the burning of single drops of fuel in an oxidizing atmosphere. *Jet Propulsion* 24(4): 245–51.

5. Law, C. K. 1982. Recent advances in droplet vaporization and combustion. *Progress Energy Combustion Sci.* 8:171–201.

6. Sirignano, W. A. 1983. Fuel droplet vaporization and spray combustion theory. *Progress Energy Combustion Sci.* 9:291–322.

7. Bachalo, W. D. 1994. In: *25th Symposium (International) on Combustion Proceedings*. Pittsburgh, PA: The Combustion Institute. 333.

8. Mashayek, F., and R. V. R. Pandya. 2003. In: *Progress Energy Combustion Sci.* 29:329.

9. Twardus, E. M., and T. A. Brzustowski. 1977. In: *Archiwum Processov Spalania* 8:347.

10. Chiu, H. H., and T. M. Liu. 1977. In: *Combustion Science Technology* 17:127.

11. Correa, S. M., and M. Sichel. 1983. In: *19th Symposium (International) on Combustion Proceedings*. Pittsburgh, PA: The Combustion Institute.

12. Marberry, M., A. K. Ray, and K. Leung. 1984. In: *Combustion Flame* 57:237.

13. Nigmatulin, R. I. 1987. *Dynamics of multiphase media*. Part 1. Moscow: Nauka Publ.

14. Dwyer, H. A., H. Nirschl, P. Kerschl, and V. Denk. 1994. In: *25th Symposium (International) on Combustion Proceedings*. Pittsburgh, PA: The Combustion Institute. 389.

15. Sivasankaran, K., K. N. Seetharamu, and R. Natarajan. 1996. In: *Int. J. Heat Mass Transfer* 39:3949.

16. Frolov, S. M., V.Ya. Basevich, V. S. Posvianskii, and V. A. Smetanyuk. 2006. Development and Implementation of Drop Evaporation Model with Regard for Spray Effect. Final Report to AVL 159236/PC.

17. Drop vaporization with regard for spray effects. *Rus. J. Chemical Physics* 23(7):49–58.

18. Frolov, S. M., V.Ya. Basevich, V. S. Posvianskii, and V. A. Smetanyuk. 2004. Drop vaporization with regard for spray effects. *Rus. J. Chemical Physics* 23(7):49–58.

19. Basevich, V. Ya., A. A. Belyaev, and S. M. Frolov. 2000. *Rus. J. Chemical Physics* 19(10):89.

20. Basevich, V. Ya., A. A. Belyaev, and S. M. Frolov. 2001. *Rus. J. Chemical Physics* 20(12):37.

21. Evlampiev, A. V., S. M. Frolov, V. Ya. Basevich, and A. A. Belyaev. 2001. *Rus. J. Chemical Physics* 20(11):21–27.

22. Frolov, S. M., V. Ya. Basevich, A. A. Belyaev, V. S. Posvianskii, and V. A. Smetanyuk. 2003. In: *Combustion and atmospheric pollution*. Eds. G. Roy, S. Frolov, and A. Starik. Moscow: TORUS PRESS. 207–13.

23. Atthasit, A., N. Doue, Y. Biscos, G. Lavergne, and A. Berlemont. 2003. In: *Combustion and atmospheric pollution*. Eds. G. Roy, S. Frolov, and A. Starik. Moscow: TORUS PRESS. 214–19.

24. Basevich, V. Ya., S. M. Frolov, and V. S. Posvyanskii. 2005. *Rus. J. Chemical Physics* 24(7):58–68.

25. Frolov, S. M., V. Ya. Basevich, A. A. Belyaev, V. S. Posvyanskii, and V. A. Smetanyuk In: Combustion and Pollution: Environmental Effect. Eds. G.D. Roy, S. M. Frolov, A. M. Starik. Moscow, Torus Press, 2005. 117–32.

26. Takei, M., H. Kobayashi, T. Niioka. Int. J. Microgravity Res. Appl. Microgravity Sci. Technol., 1993, VI/3:184–87.

27. Niioka T., Kobayashi H., Mito D. IVTAM Symp. on the Mechanics and Combustion of droplet and Sprays, Tainan, Dec. 1994, p.367.

28. Sokolik A.S., Basevich V.Ya. J. Physical Chemistry, 1954, Vol. 28, No.11, p. 1935.

29. Tanner F.X. SAE Techn. Paper Series, 2003-01-1044.